ISSN 0915-633X

NATIONAL INSTITUTE FOR FUSION SCIENCE

Effect of the Resistive Wall on the Growth Rate of Weakly Unstable External Kink Mode in General 3D Configurations

M.S. Chu, K. Ichiguchi

(Received - Apr. 4, 2005)

NIFS-812 May 2005

RESEARCH REPORT
NIFS Series

TOKI, JAPAN

Effect of the Resistive Wall on the Growth Rate of Weakly Unstable External Kink Mode in General 3D Configurations

M. S. Chu,[a)] K. Ichiguchi
National Institute for Fusion Sciences
Toki 509-5292, Japan

[a)]Permanent Address: General Atomics,
San Diego, California 92186-5608 USA

Abstract

Formulation of a method for the systematic computation of the growth rate of the weakly unstable RWM in 3D configurations by using results from ideal stability codes is presented. It is shown that the growth rate of the RWM is approximately given by the rate at which the available free energy for the ideal external kink mode can be dissipated by the resistive wall. The eigenfunction is also approximated by that of the external kink mode. This formulation is demonstrated by coupling to the ideal MHD code KSTEP with computation of the dissipation on the resistive wall. Results of the stability of the RWM in LHD plasmas and discussion on the validity and improvement to the computation are also included.

Key Words :
Resistive Wall Mode, 3D MHD Stability, Formulation and Application to LHD

*This is a preprint of an article to be published in the journal Nuclear Fusion, a publication of the International Atomic Energy Agency, : http://www.iop.org/ej/nf.

1 Introduction

The external kink mode has long been recognized as being one of the most serious instabilities that affect the plasma confinement, sometimes even to the extent of destroying the plasma. Therefore control of the external kink mode is one of the most important topics in confinement physics. The growth rate of the external kink mode is usually a fraction of the inverse of Alfven transit time $(\tau_A)^{-1}$, up to $10^6/sec$. This fast rate is outside the range of being feasible for plasma control. The external kink mode can be stabilized by the presence of a near-by perfect conducting wall. When the resistivity of the wall is taken into account, the external kink mode is changed into the resistive wall mode (RWM) [1]. It's growth rate then reduces to the inverse of the flux diffusion time through the resistive wall $(\tau_w)^{-1}$, usually slower than $10^3/sec$. With its growth rate slowed down, the RWM has been demonstrated[2] to be stabilized either by plasma rotation [3] or magnetic feedback[4, 5]. In configurations without toroidal symmetry, plasma rotation is relatively small and is not expected to be able to stabilize the RWM. Therefore, it is expected that we would have to rely on magnetic feedback to stabilize the RWM in these configurations. Before undertaking the task of design for feedback control of the RWM, we need to study the growth rate of the RWM in these configurations. The growth rate of the resistive wall mode in these 3D configurations is one of the main focus of the present work.

In experiments on DIII-D, the structure of the RWM has been found to be well represented by the eigenfunction obtained from ideal external kink computations with the resistive wall at infinity. [6, 7]. It has also long been conjectured that the structure of the resistive wall mode should be the same as that of the external kink. In this work, we present a systematic justification of this conjecture and show that a sufficient condition for the RWM to share the same eigenfunction as the ideal external kink is when the RWM is weak, or the plasma is close to the unstable no wall limit and far from the stable ideal wall limit. This is the second purpose of the present work.

The formulation for determining the growth rate of the RWM in general plasma configuration has been given by Chu et al[8]. For toroidally symmetric configurations, this formulation has been implemented by coupling the DCON[9] ideal MHD stability code with the extended VACUUM code[10, 11] and other software packages. This provided a general tool for determining the growth rate of the RWM in axi-symmetric confinement devices.

Conventional stellarators[12, 13] are non-axisymmetirc, usually have negligible toroidal current and have been known to be free of external kink modes. However, advanced compact stellarators[14, 15] at reactor density and temperature conditions do produce non-negligible toroidal bootstrap current and are not immune to the external kink mode. In practice, the external kink mode can only be controlled when they are weakened by the presence of nearby external resistive conductors. Therefore, it is natural to ask: is there a reliable method to study the effect of the nearby resistive wall on the growth rates of the RWM for weakly unstable 3D configurations? At present, there are well-established computer codes that can study the stability of the external kink mode in 3D geometry. Three of these are the Terpsichore[16] ,the CAS3D[17] and the KSTEP code[18, 19, 20]. These codes have been routinely employed to study the stability of the external kink mode in 3D configurations. We note further that Merkel et al. has recently generalized the CAS3D code to calculations include the RWM[21] regime. This work represents a first systematic treatment for the RWM in fully 3D configuration. This work shares much similarity to the original work proposed in Ref. [8] to connect with the usual MHD codes. The advantage of this is to bring us back to the basic concepts of free energy and dissipation and also as a complement to the work of Merkel et al.[21] In the present work, on the other hand, we adopt yet another alternative

route. We look for an intermediate approximate solution which can be easily obtained by extending existing 3D ideal MHD codes. It is natural to seek coupling with these codes in determining the growth rate of the RWM.

In this work, we make progress in this direction by making a connection between the existing ideal MHD stability codes with the diffusion of flux on the external resistive wall. This enables us to provide an approximate yet systematic answer to the change in growth rate of the unstable mode from the external kink mode to that of the RWM. The formulation of this approach is given in section II. In this section, we have also proved that the structure of the RWM should indeed be given by that of the ideal external kink. As a first demonstration, we apply this method to the study of the stability of the RWM in LHD on results of the stability of the external kink mode obtained from the KSTEP code [18, 19, 20]. Results of this application is shown in section III. A brief discussion is given in Section IV. Three appendices are also included. In Appendix A, we discuss the dissipation functional in the resistive wall. In Appendix B, we use known analytic solvable cases of RWM in equilibria with one dimensional symmetry to clarify the nature of the approximation proposed in the present method. We showed that the method is valid if the plasma is close to the unstable no wall limit but far from the stable ideal wall limit. We also make suggestions on reasonable corrections to the approximation. In Appendix C, we give the expression employed in KSTEP code to compute, including toroidal correction effects, the perturbed magnetic field in the plasma.

2 Formulation for the Computation of the Growth Rates of the RWM in 3D Configurations by Coupling with Existent Ideal MHD Codes

In this section, we provide the formulation for the systematic study of the effect of the resistive wall on the growth rate of the RWM in weakly unstable 3D configurations. Starting from the general formulation of Ref. [8], we show that a good approximate answer can be obtained by the balance of two quantities. The first quantity is the total amount of free energy available to drive the external kink mode. This quantity is obtained by ideal MHD codes with the external wall at infinity. We represent it as $-(\delta W_p + \delta W_{v\infty})$. Here δW_p is the potential energy of the plasma, and $\delta W_{v\infty}$ is the perturbed vacuum energy with the wall at inifinity. The second quantity is D_w, the energy dissipated by the resistive wall. D_w is in turn the product of two factors. The first factor is the growth rate γ of the RWM in units of the resistive wall time τ_w, i.e. $\gamma\tau_w$. The second factor is the energy dissipation form factor $\bar{D}_w$. This form factor depends on the perturbed magnetic field at the resistive wall. Thus our result is given as

$$\gamma\tau_w \simeq -\frac{\delta W_p + \delta W_{v\infty}}{\bar{D}_w} \tag{1}$$

It is the purpose of this section to provide a derivation of Eq. (1). We start from the exact formulation given by the general expression stated in Ref. [8] and consider the situation without feedback. It is shown that the general energy conservation relationship ($\delta W_g = 0$) for perturbation in plasma surrounded by a resistive wall is

$$\delta W_g \equiv \delta W_p + \delta K + \delta W_v + D_w = 0 \tag{2}$$

In Eq. (2), δK is the perturbed plasma kinetic energy. All of the energy expressions in here are well known[22] excerpt D_w, which is the Ohmic dissipation by the resistive wall. For

completeness, we provide in Appendix A a brief description of the expression for D_w. δW_g is a bilinear functional of the perturbed plasma displacement $\vec{\xi}$ in the plasma and $\delta\vec{B}$ in the vacuum region. In the vacuum region, the perturbed magnetic field is related to the perturbed magnetostatic potential χ by

$$\vec{\delta B} = \vec{\nabla}\chi \tag{3}$$

δW_g has been shown to be self-adjoint with respect to the perturbed quantities $(\vec{\xi}, \delta\vec{B})$. We indicate this property of δW_g explicitly as

$$\delta W_g(\vec{\xi^\dagger}, \delta\vec{B}^\dagger; \vec{\xi}, \delta\vec{B}) = \delta W_g(\vec{\xi}, \delta\vec{B}; \vec{\xi^\dagger}, \delta\vec{B}^\dagger) \tag{4}$$

In Eq. (4), the adjoint quantities are indicated by the superscript †. Eq. (2) is also variational with respect to $\vec{\xi}$ and χ, with the Euler equations

$$L_{MHD}\vec{\xi} = 0 \tag{5}$$

in the plasma region. In Eq. (5), L_{MHD} is the usual linear ideal MHD operator[**?**]. and

$$\nabla^2\chi = 0 \tag{6}$$

in the vacuum region. The boundary conditions are that the perturbed magnetic field perpendicular to the boundary surfaces (both between the plasma and vacuum, and between the vacuum and the resistive wall) should be continuous across the boundary. An important consequence is that any $(\vec{\xi}, \chi)$ that satisfies Eqs. (5) and (6) and with δB_n continuous across the appropriated boundaries will satisfy

$$\delta W_g(\vec{\xi'}, \delta\vec{B}'; \vec{\xi}, \delta\vec{B}) = 0 \tag{7}$$

for any $(\vec{\xi'}, \chi')$ and is not limited to the adjoint of $(\vec{\xi}, \chi)$.

The equilibrium properties of the plasma enter into Eq. (2) parametrically. This set of parameters we denote by $\{\alpha\}$. In here $\{\alpha\}$ can include such quantities as the total plasma current, pressure and profile parameters etc. We note that Eq. (2) has two major reduced situations. The first is the case of the absence of the external resistive wall. δW_g is reduced to δW_I of the usual ideal MHD.

$$\delta W_I \equiv \delta W_p + \delta K + \delta W_v = 0 \tag{8}$$

In this case, the dissipation of the resistive wall plays no role in determining the growth rate of the instability. The second reduced situation is the case of the RWM with a finite but small resistivity on the external wall. In this case, the growth rate is so slow, that the plasma kinetic energy is negligible. δW_g is reduced to δW_r for studying the RWM.

$$\delta W_r \equiv \delta W_p + \delta W_v + D_w = 0 \tag{9}$$

Eqs. (8) and (9) reveal the important fact that the ideal external kink and the RWM share the same free energy source. In these two equations, all terms except δW_p are positive definite. So both of these modes are driven by the free energy from the plasma that is not counterbalanced by an infinite external vacuum region. For the ideal external kink, this free energy is transformed into the kinetic energy of the plasma; whereas for the RWM this energy is transformed into the joule heat on the resistive wall. A small imbalance between δW_p and δW_v would result in small δK or small D_w. Because the growth rate enters δK quadratically,

and also because it is in units of the inverse Alfven transit time, the resultant ideal growth rate could still be physically un-tolerable. The growth rate enters into D_w linearly, with its basic time scale determined by τ_w. A small net free energy resultant from the imbalance between δW_p and δW_v will result in a slow growth rate of the RWM (so long as it is stable to the ideal mode with the resistivity of the wall set to zero).

There is one situation in which the ideal external kink and the RWM share the same eigenfunction. That is when the plasma is marginally stable to the ideal external kink mode with the wall at infinity, or for the RWM with the resistive wall at any location. We denote this equilibrium as given by the parameters $\{\alpha_0\}$, or

$$\delta W_I(\alpha_0) = \delta W_p(\vec{\xi}_0^\dagger, \vec{\xi}_0; \alpha_0) + \gamma_0^2 \tau_A^2 \delta \bar{K}(\vec{\xi}_0^\dagger, \vec{\xi}_0; \alpha_0) + \delta W_v(\delta \vec{B}_0^\dagger, \vec{\delta} B_0; \alpha_0) = 0 \tag{10}$$

In Eq. (10), we indicated that the equilibrium parameters are given by $\{\alpha_0\}$. We have also taken out the explicit frequency dependence of δK and note that $\gamma_0 = 0$. Next we consider a different (unstable) plasma equilibrium specified by

$$\{\alpha\} = \{\alpha_0\} + \{\alpha_1\} \tag{11}$$

with $\{\alpha_1\}$ denoting the small change in equilibrium parameters. Then the ideal stability functional is given by

$$\delta W_I(\alpha) = \delta W_p(\vec{\xi}_\alpha^\dagger, \vec{\xi}_\alpha; \alpha) + \gamma^2 \tau_A^2 \delta \bar{K}(\vec{\xi}_\alpha^\dagger, \vec{\xi}_\alpha; \alpha) + \delta W_v(\delta \vec{B}_\alpha^\dagger, \vec{\delta} B_\alpha; \alpha) = 0 \tag{12}$$

We assume that the perturbation to the equilibrium is small. (In particular, it does not give rise to a large perturbation to the displacement of the unstable mode at the plasma edge.) Then the perturbation to the mode structure is also small, i.e.

$$\vec{\xi}_\alpha = \vec{\xi}_0 + \delta\vec{\xi}_1 + ... \tag{13}$$

$$\delta\vec{B}_\alpha = \delta\vec{B}_0 + \delta\vec{B}_1 + ... \tag{14}$$

In Eqs. (13) and (14), $\delta\vec{\xi}_1$ and $\delta\vec{B}_1$ are first order quantities in $\{\alpha_1\}$. We note that in Eq. (12) $\gamma^2\tau_A^2$ is a first order quantity. We may substitute Eqs. (13) and (14) into Eq. (12). Each of the energy expressions can be expanded to include zeroth, first, second, and ... order quantities in $\{\alpha_1\}$. We express this as

$$\delta W_I(\alpha) = \delta W_I^0(\alpha) + \delta W_I^1(\alpha) + ... \tag{15}$$

By assumption, to the lowest (zeroth) order,

$$\delta W_I^0(\alpha) = \delta W_I(\alpha_0) \tag{16}$$

To the first order,

$$\delta W_I^1(\alpha) = \delta W_p^1(\vec{\xi}_\alpha^\dagger, \vec{\xi}_\alpha; \alpha) + \gamma^2 \tau_A^2 \delta \bar{K}(\vec{\xi}_0^\dagger, \vec{\xi}_0; \alpha_0) + \delta W_v^1(\delta \vec{B}_\alpha^\dagger, \vec{\delta} B_\alpha; \alpha) = 0 \tag{17}$$

where

$$\delta W_p^1(\vec{\xi}_\alpha^\dagger, \vec{\xi}_\alpha; \alpha) = \delta W_p(\delta\vec{\xi}_1^\dagger, \delta\vec{\xi}_0; \alpha_0) + \delta W_p(\delta\vec{\xi}_0{}^\dagger, \delta\vec{\xi}_1; \alpha_0) + \delta W_p(\vec{\xi}_0^\dagger, \vec{\xi}_0; \alpha_1) \tag{18}$$

, and

$$\delta W_v^1(\delta\vec{B}_\alpha^\dagger, \delta\vec{B}_\alpha; \alpha) = \delta W_v(\delta\vec{B}_1^\dagger, \delta\vec{B}_0; \alpha_0) + \delta W_v(\delta\vec{B}_0{}^\dagger, \delta\vec{B}_1; \alpha_0) + \delta W_v(\delta\vec{B}_0^\dagger, \delta\vec{B}_0; \alpha_1) \tag{19}$$

. We notice that because δW_I in Eq. (8) and therefore Eq. (10) is self-adjoint, we know from the orthogonality property Eq. (7) that

$$\delta W_p(\vec{\xi}_0^\dagger, \delta\vec{\xi}_1; \alpha_0) + \delta W_v(\delta\vec{B}_0^\dagger, \delta\vec{B}_1; \alpha_0) = 0 \tag{20}$$

In Eq. (20) we used explicitly the fact that $\gamma_0 = 0$. By use of Eq. (20) and its adjoint expression, we obtain

$$\delta W_I^1(\alpha) = \delta W_p(\vec{\xi}_0^\dagger, \vec{\xi}_0; \alpha_1) + \gamma^2\tau_A^2\delta\bar{K}(\vec{\xi}_0^\dagger, \vec{\xi}_0; \alpha_0) + \delta W_v(\delta\vec{B}_0^\dagger, \delta\vec{B}_0; \alpha_1) = 0 \tag{21}$$

The importance of this relationship is that in the total eigenfunction $\{\vec{\xi}, \delta\vec{B}\}$, we need only the portion $\{\vec{\xi}_0, \delta\vec{B}_0\}$ from the unperturbed equilibrium . Therefore, we may evaluate the ideal growth rate by

$$\gamma^2\tau_A^2 \simeq \frac{\delta W_p(\alpha_0) + \delta W_v(\alpha_0) - \delta W_p(\vec{\xi}_0^\dagger, \vec{\xi}_0; \alpha) + \delta W_v(\delta\vec{B}_0^\dagger, \delta\vec{B}_0; \alpha)}{\delta\bar{K}(\alpha_0)} \tag{22}$$

Up to now, in Eq. (22) only the eigenfunction of the unperturbed equilibrium is used. This expression is correct up to first order in $\{\alpha_1\}$. In practice, because of the marginal stability condition of Eq. (10), and because of the relationship Eq. (13), we can also evaluate the growth rate as

$$\gamma^2\tau_A^2 \simeq -\frac{\delta W_p(\alpha) + \delta W_v(\alpha)}{\delta\bar{K}(\alpha)} \tag{23}$$

We know that this is actually an exact expression. We followed a complicated route to prove that it is correct at least up to first order in $\{\alpha_1\}$. Our purpose is to relate it to the situation of the RWM.

Next we consider the situation when a resistive wall is present. (We implicitly assume that if the resistive wall were ideally conducting, the plasma would be stable to the ideal external kink.) We may first examine the expression δW_r given in Eq. (9) for the RWM for the equilibrium which is marginally stable. This is written as

$$\delta W_r(\alpha_0) = \delta W_p(\vec{\xi}_0^\dagger, \vec{\xi}_0; \alpha_0) + \gamma_{0r}\tau_w\bar{D}_w(\delta\vec{B}_0^\dagger, \delta\vec{B}_0; \alpha_0) + \delta W_v(\delta\vec{B}_0^\dagger, \delta\vec{B}_0; \alpha_0) = 0 \tag{24}$$

In Eq. (24), we again took out the explicit frequency dependence of D_w. From the assumption of marginal stability, we know that $\gamma_{0r} = 0$. We also note that because of the assumption of marginal stability, we have used the same eigenfunctions in Eq. (24) as in Eq. (10). Next, for the equilibrium specified by the parameter set in Eq. (11), the functional δW_r satisfies

$$\delta W_r(\alpha) = \delta W_p(\vec{\xi}_{\alpha r}^\dagger, \vec{\xi}_{\alpha r}; \alpha) + \gamma_r\tau_w\bar{D}_w(\delta\vec{B}_{\alpha r}^\dagger, \delta\vec{B}_{\alpha r}; \alpha) + \delta W_v(\delta\vec{B}_{\alpha r}^\dagger, \delta\vec{B}_{\alpha r}; \alpha) = 0 \tag{25}$$

In Eq. (25), we emphasize that the eigenfunction given by $\{\vec{\xi}_{\alpha r}, \delta\vec{B}_{\alpha r}\}$ is now different from that of the ideal MHD eigenfunctions $\{\vec{\xi}_\alpha, \delta\vec{B}_\alpha\}$ in Eq. (12). However, $\{\vec{\xi}_{\alpha r}, \delta\vec{B}_{\alpha r}\}$ can still be related to the set $\{\vec{\xi}_0, \delta\vec{B}_0\}$ by the relationships

$$\vec{\xi}_{\alpha r} = \vec{\xi}_0 + \delta\vec{\xi}_{1r} + ... \tag{26}$$

$$\delta\vec{B}_{\alpha r} = \delta\vec{B}_0 + \delta\vec{B}_{1r} + ... \tag{27}$$

In Eqs. (26) and (27), $\delta\vec{\xi}_{1r}$ and $\delta\vec{B}_{1r}$ are also of first order in $\{\alpha_1\}$. We may now follow exactly the same development presented above from Eq. (15) to Eq. (23) to show that to first order in $\{\alpha_1\}$

$$\gamma_r\tau_w \simeq -\frac{\delta W_p(\alpha) + \delta W_v(\alpha)}{\bar{D_w}(\alpha)} \tag{28}$$

In Eq. (28), the eigenfunction computed by the ideal MHD code for the external kink mode with the equilibrium parameter $\{\alpha\}$ is used. An important point to note is that contrary to Eq. (23), which is exact, Eq. (28) is only approximate.

The present derivation shows that we may utilize the results from general ideal MHD computations to compute an approximate growth rate of the RWM so long as the kinetic energy of the ideal MHD mode is small compared with the potential energy of the plasma and that of the vacuum region. What is needed is the deviation of the potential energy $\delta W_p + \delta W_v$ from the marginally stable plasma and the additional computation of the value of the dissipation functional $D_w(\alpha)$ due to the perturbed magnetic field in the vacuum region. Intuitively, the result given in Eq. (28) is very appealing. It just states that the growth rate is determined by the rate at which the free energy can be dissipated by the resistive wall. We would like to emphasize that the present formula is only approximate. The approximation is in two parts: first the plasma eigenfunctions are expected to be (slightly) different for the ideal instability and the RWM; second, the vacuum energy is also modified by the change in the plasma eigenfunction and also the presence of the eddy currents on the resistive wall. The present derivation shows that these modifications give rise to higher order corrections to the value of the computed growth rate of the RWM given in Eq. (28). A more complete and accurate solution would have to follow the procedure given in the work of Chu et al[8].

A consequence of the present derivation is that when the RWM is weak, we expect its mode structure, including the magnetic field in the vacuum region, to be given by that of the ideal external kink mode with the wall at infinite. We give in Appendix B a more quantitative discussion on this notion of the weakness of the RWM. We show that a RWM is weak when the plasma is close to the unstable no wall limit and far from the stable ideal wall limit.

3 Numerical Implementation and Application to LHD

The formulation presented in Section II is implemented by coupling a computation of D_w to results from the KSTEP code[18, 19, 20]. For a given 3D equilibrium computed by the VMEC code[23], the KSTEP code computes its free-boundary stability for given position of the ideal wall. The KSTEP code is an ideal stability code based on the stellarator expansion method. Originally, Anania and Johnson developed the STEP code by strictly employing the stellarator ordering of $a/R_0 \sim (B_\delta/B_0)^2 << 1$[18]. Nakamura et al. included the higher order terms in the formalism of the stellarator expansion to apply the method to medium aspect ratio stellarators such as LHD, and developed the KSTEP code as an extension of the STEP code[19, 20]. The RWM is expected to be present in equilibria that are unstable to the external kink mode with the wall at infinity and stable with the wall being ideal. We first obtain the unstable eigenvalues $\gamma^2\tau_A^2$ and the perturbed magnetic fields at the plasma edge δB_p with the external wall at infinity. In here the subscript p denotes the component perpendicular to the plasma boundary. δB_p is used to compute the perturbed perpendicular magnetic fields δB_w at the resistive wall. This is best accomplished by using the Green's function method. This method is generally used for the vacuum region and is also the method used in KSTEP; except that the original KSTEP did not compute δB_w and also δB_p. In this work, we added this additional computation a posteriori after the KSTEP computation for δB_p. δB_w is then used in turn to compute the dissipation functional in Eq. (1). We note that if δB_w and the dissipation were computed together in KSTEP, then the validity is not restricted only to weakly unstable RWM and would be valid for RWM with arbitrary strength.

We used this method to study the effect of resistive wall on the stability of the external

kink in LHD. The LHD is an $l = 2$ heliotron with 10 toroidal field periods. It has a pair of helical windings with the major radius of $3.9m$. It can be heated by neutral beam injection (NBI), electron cyclotron resonance heating (ECRH), and ion cyclotron resonance heating (ICRF). In its normal operation, with net zero toroidal current, it has achieved high β value of up to 4% without the observation of any external kink instability [24]. We have to choose special parameter ranges for the VMEC[23] equilibrium code , which are different from those employed normally in LHD, to generate equilibria that are suitable for the study of stability of external kink modes. The applicability of the KSTEP code for the modes with $n \leq 3$ in the LHD configuration was confirmed by the benchmark test with the full 3D codes of the CAS3D and the TERPSICHORE[25].

We concentrate on low β plasmas in the configuration with $R_{ax} = 3.75m$ to isolate the source of instability to be due to the toroidal plasma current. In this case, the relevant equilibria that are unstable to the external kink mode with the wall at infinity, but stable with an ideal wall close to the plasma have a very limited range of toroidal plasma current. For toroidal field $B_t = 1T$, it is from 130kA to $135kA$. For currents smaller than $130kA$, the plasma is stable to the external kink mode; whereas for current higher than $137kA$, the plasma is unstable even with the wall right on the plasma surface. The overview of this behavior of the stability of the external kink mode is shown in Fig.1

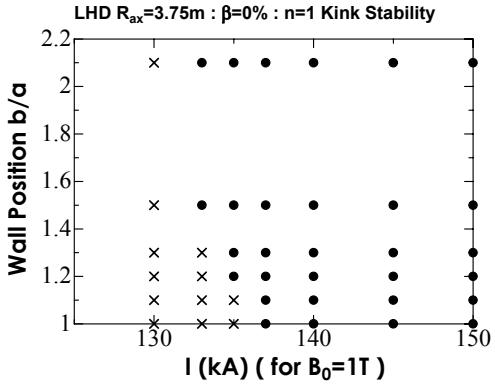

Figure 1: Stability diagram of the n=1 ideal external kink mode in LHD with major radius at $3.75m$, $\beta = 0\%$ and toroidal field of $1T$. The horizontal axis is the total plasma current. The vertical axis is the average wall radius b relative to the average plasma radius a. Stable equilibria are marked by blue cross and unstable ones are marked by red dot. The blue cross are cases in which RWMs are expected.

In Fig.1, the $n = 1$ stability of the $\beta = 0\%$ LHD equilibria with major radius $R_{ax} = 3.75m$ and different amount of total plasma current I are indicated with different external wall positions given by the parameter b/a. In these equilibria, a parabolic current density profile is used. Here, n is the toroidal mode number. a is the average plasma radius which is obtained from the stellarator expansion method. In this configuration, a is approximately $.6meter$. The external wall has been approximated to be a torus with a circular cross section with minor radius b (See Fig.2.) We note that the actual plasma cross-section is non-circular and maintain its relative shape and location with respect to the helical winding. The actual external chamber is also not a torus with circular cross-section but maintain a definite relationship with the plasma and the external coils. Near the helical midplane at the vertically elongated poloidal cross-section, the inboard-side resistive external chamber is quite close to the plasma, with an approximate ratio of the radii b/a of around 1.1. However, in the direction at 90 degrees relative to the helical midplane, the chamber dimension is quite far away from the

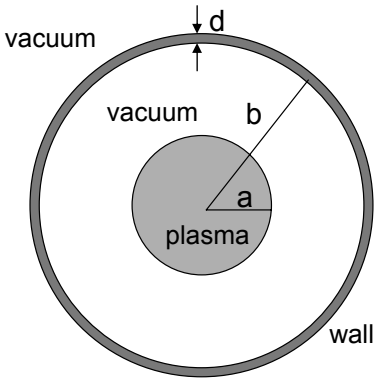

Figure 2: Schematic view of the positions of the plasma and the wall

plasma. It can have a ratio of the radii b/a beyond 2.0. Here we have chosen to have the ratio of b/a range from 1.0 to 2.2. In Fig.1, all plasmas with current settings with current larger than 130kA is unstable to the external kink with the wall at infinity. The ideal wall location at which the external kink can be stabilized is given by the blue cross, and indicated by a red dot otherwise. Only the external kinks in discharges indicated by the blue cross can have their growth rates reduced by the presence of the resistive wall.

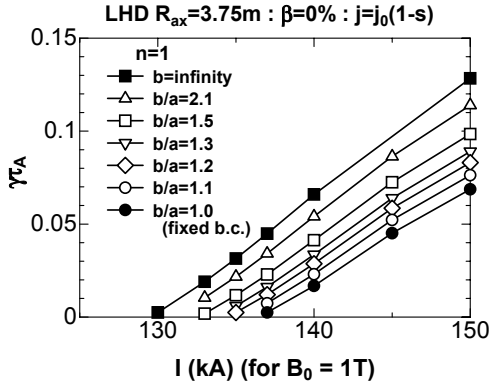

Figure 3: Growth rate γ of the n=1 ideal external kink in LHD in units of inverse Alfven transit time τ_A^{-1} for different discharge currents. Different symbols are used for lines with different locations b/a of the external wall. The range of current that can be affected by the presence of the external wall is between the intersects of the $b/a = \infty$ line and that of the corresponding $b/a = constant$ line.

The growth rates of the unstable ideal external kink in units of Alfven transit time $\gamma\tau_A$ of the above set of equilibria are given in Fig.2. It is interesting to note that the range of growth rates in which the resistive wall would have an effect is very small indeed. In Fig.2, for current of $135kA$ and with the wall at infinity, the growth rate is given by $\gamma\tau_A = 3\%$. At this value, $\gamma^2\tau_A^2 \sim 10^{-3}$. But this equilibrium can not be stabilized by the ideal wall. Equilibria that can be stabilized by the ideal wall has maximum $\gamma^2\tau_A^2 \sim 10^{-4}$.

For completeness, we show the profiles of the rotational transform as a function of the normalized poloidal flux Ψ in Fig.3 and the profiles of the plasma displacement in Fig.4. It is seen that with increase of the plasma current, the profiles of the rotational transform is lifted. At $150kA$, the whole profile is lifted above 1.. There is also a corresponding change in

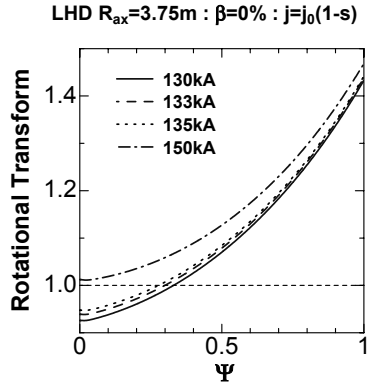

Figure 4: Variation of the rotational transform across the flux surface. It is seen that the RWM relevant equilibria studied here ($130kA \leq I \leq 135kA$) has a very limited variation in the rotational transform profile. They are also characterized by the presence the crossing of the $\iota = 1$ line. At $I \geq 150kA$, the rotational transform is larger than 1 across the plasma cross-section.

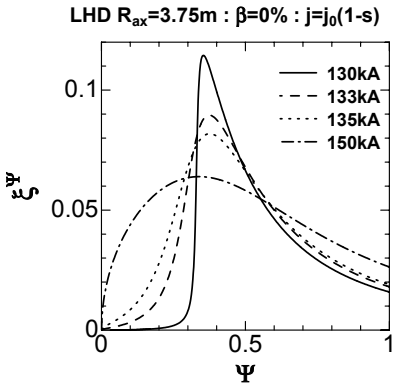

Figure 5: Variation of the plasma displacement of the unstable ideal kink mode across the flux surface. It is seen that for the RWM relevant equilibria studied here the displacements are characterized by the sharped peak around the singular surface of the $\iota = 1$. At $I \geq 150kA$, this sharp peak is rounded out.

the profiles of the plasma displacement. The characteristic sharp peak of the displacement at location near the internal resonant surface of $\iota = 1$ is broadened. The plasma displacement is dominated by the component with poloidal mode number $m = 1$.

We show in Fig.5 the computed growth rate of the RWM for those cases where the external kink is stabilized if the external wall were ideal. The blue curve is for current of $130kA$, green for $133kA$ and red for $135kA$. The resistivity of the external wall has been taken to be $87 \times 10^{-8}\Omega \cdot m$ and thickness of $15mm$. For $b/a = 2$ or with wall radius at $1.2m$, the diffusion time constant of the resistive wall is approximately

$$\tau_w = \frac{\mu_0 \cdot b \cdot db}{\eta} = 31.5msec \tag{29}$$

We see that as the wall radius increases, the growth rate of the RWM increases. This is due to the decrease in dissipation at the resistive wall, despite the increase in the resistive wall time constant given by Eq. (29). When the external kink is stronger, the growth rate of the RWM is also larger.

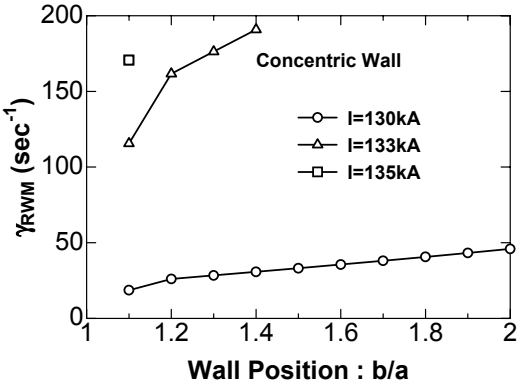

Figure 6: Computed growth rate of the RWM as a function of the location of the resistive wall. It is seen that this growth rate increases with the radius of the external wall and are also larger for equilibria that are more unstable to the external kink mode.

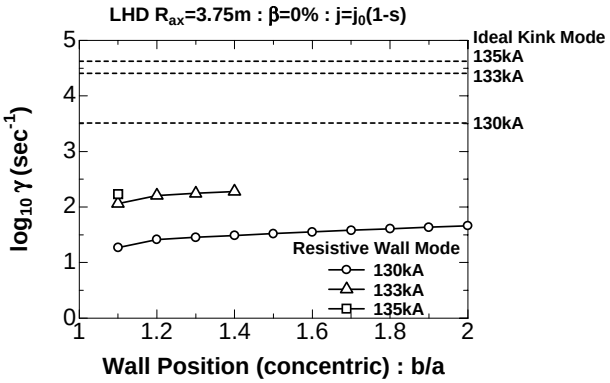

Figure 7: Computed growth rates of the RWM as a function of the location of the resistive wall shown together with the computed growth rates of the ideal external kink from KSTEP with the wall at inifinity. It is seen that the growth rates of the RWM are indeed much lower than that of the ideal external kink

We show in Fig.6 the comparison of the computed growth rates of the RWM for the cases shown in Fig.5 together with the growth rates of the ideal external kink with the wall at inifinity. The vertical axis is in logarithmic scale. We see that the growth rates of the RWM is indeed much lower than that of the ideal external kink.

In the calculation of the KSTEP code of the present analysis, we employed the 22 poloidal modes in the range of $-7 \leq m \leq 14$. This choice is sufficient for the present case because the amplitude of the mode except $m = 1$ of the kink mode is negligible compared with that with $m = 1$. We also examined the stability for the external kink mode with $n = 2$ and 3 with the wall at infinity. The growth rates of the both modes are less than that of the $n = 1$ mode.

4 Conclusion

In this work, we presented the formulation of a method for the systematic computation of the growth rate of the RWM in weakly unstable 3D configurations by using results from ideal stability codes. This method is based on Eq. (1). It states that the growth rate of the

RWM is proportional to the rate at which the free energy available (for the ideal external kink mode with the wall at infinity) can be dissipated by the resistive wall. We note that this is an alternative method and complements the work by Merkel et al.[21]. By relying on the concepts of energy and dissipation, the method is readily connected with other MHD codes and provides an independent and useful method of studying the physics of RWM. In Section II, we provided a derivation and justification of this expression. It is shown that this expression is valid when the external kink has relatively small amount of free energy. In this case, the eigenfunction of the resistive wall mode can also be approximated by that of the ideal external kink. In this formulation the ideal MHD codes provide information about the amount of free energy available in terms of $-(\delta W_p + \delta W_v)$ with the wall at infinity. The corresponding perturbed magnetic field at the location of the resistive wall can then be used to evaluate the rate of energy dissipation in the resistive wall to obtain the growth rate of the RWM. In Appendix B, we further clarify the notion of the weakness of the RWM to mean the plasma as being close to the unstable no wall limit and far from the stable ideal wall limit. In section III, this formulation is demonstrated by coupling to the ideal MHD code KSTEP to study the stability of the RWM in LHD plasmas. It is found that in terms of plasma current, a very limited range of the plasma equilibria can have its external kink mode affected by the presence of the resistive wall, i.e. the plasma quickly transits from being stable to the external kink mode to being unstable even with the wall right on the plasma. Nevertheless, we have demonstrated that the proposed method can be used to evaluate the growth rate of the RWM in any 3D configurations readily. The growth rate in the advanced stellarators can also be calculated by employing full 3D codes such as CAS3D and TERPSICHORE instead of the KSTEP code.

We acknowledge discussion with Prof. T. Hayashi and other staffs at NIFS. One of us (MSC) acknowledges hospitality of NIFS where this research is performed. We also thank Dr. J.L. Johnson and Dr. Y. Nakamura for the usage of the KSTEP code. We would also like to thank the referee in pointing us to Ref. [21] on the status of the CAS3D code. Work partially supported by U.S. DOE under Grant No. DE-FG03-95ER54309. This work is also supported by the Grant-in-Aid for Scientific Research (C) 13680572 of the Japan Society for the Promotion of Science.

A General Expression for the Dissipation Function in the Resistive Wall D_w

In this appendix, we give the general expression for the dissipation function D_w and its relation to the perpendicular magnetic field δB_w at the resistive wall. We use the thin wall approximation in which δB_w is assumed to be constant across the resistive wall. The resistive wall is taken to be thin, but with variable resistivity η and thickness db over its surface. The general expression of for D_w given in Ref. [8] is

$$D_w = \frac{1}{2\mu_0} \int_w dS(\chi_+^\dagger - \chi_-^\dagger)\delta B_w \tag{30}$$

In Eq. (30), dS is the surface area element of the resistive wall, subscript $(+,-)$ represents (outside,inside) edge of the resistive wall. In here, D_w mainly states that this is the amount of energy input into the resistive wall region. The distribution of currents on the resistive wall depends on the property such as η and d of the resistive wall. In the thin wall approximation,

the current density on the resistive wall can be represented as

$$\vec{j} = \vec{\nabla} z \times \vec{\nabla} K \tag{31}$$

In Eq. (31), z is a coordinate across the resistive wall. For instance, we may take $z = (0, 1)$ to be at the (inside,outside) edge of the resistive wall. Here, K is the stream function for the perturbed current density $\vec{j}$. In the thin wall approximation, we may take the current potential K to be varying only over the surface of the resistive wall and not depending on z. In the resistive wall,

$$\vec{\nabla} \times \delta B = \mu_0 \vec{j} = \mu_0 \vec{\nabla} z \times \vec{\nabla} K \tag{32}$$

By use of the Stokes theorem and integrate Eq. (32) over a loop with two sides anchoring on the inside and outside edge of the resistive wall, jumping across the thin wall to close the loop and enclosing a surface area in the wall which current $\vec{j}$ flows through, we may derive that

$$[\chi]_-^+ = [\int \vec{\delta} B \cdot dl]_-^+ = \mu_0 \int K dz \tag{33}$$

In Eq. (33), dl is line element along the loop at the surface edge of the resistive wall, $[]_-^+$ stands for jump of the quantity from the inside edge to the outside edge of the surface of the resistive wall. By use of Eq. (3), we arrive at an equivalent expression for the D_w

$$D_w = \frac{1}{2} \int_w dS dz K \delta B_w \tag{34}$$

By combining the Ohm's law and the induction equation, the perturbed magnetic field in the resistive wall may be related to K as

$$-\frac{\partial \delta \vec{B}}{\partial t} = \vec{\nabla} \times (\eta \vec{\nabla} z \times \vec{\nabla} K) \tag{35}$$

The component of Eq. (35) normal to the resistive wall then gives

$$\vec{\nabla}_s \cdot \eta (\vec{\nabla} z)^2 \vec{\nabla}_s K = -\gamma \delta B_w \mid \vec{\nabla} z \mid \tag{36}$$

In Eq. (36), the symbol $\vec{\nabla}_s$ denotes the component of $\vec{\nabla}$ on the surface of the resistive wall. The left hand side of equation is an operator which operates on K. It is self-adjoint and is a property of the resistive wall. This operator defines a system of electromagnetic normal modes on the resistive wall and has a complete set of eigenfunctions K_i with distinct eigenvalues ω_i that are orthogonal to each other.

$$\vec{\nabla}_s \cdot \eta (\vec{\nabla} z)^2 \vec{\nabla}_s K_i = -\omega_i K_i \mid \vec{\nabla} z \mid \tag{37}$$

The K_i thus defined are the electromagnetic dissipation eigenfunction of the resistive wall with ω_i being the dissipation rate. Thus the meaning of Eq. (36) is that these dissipation eigenfunction are excited by the changing magnetic field $\gamma \delta B_w$ that is penetrating through the resistive wall. The K_i's satisfies

$$\int_w dV \eta (\vec{\nabla} z)^2 \vec{\nabla} K_i \cdot \vec{\nabla} K_j^\dagger = \delta_{ij} \omega_i \int_w dV K_i K_j^\dagger \mid \vec{\nabla} z \mid \tag{38}$$

Thus we may expand the current potential K in terms of these dissipation eigenfunctions

$$K = \sum_i \alpha_i K_i \tag{39}$$

The coefficients α_i is related to the perturbed normal magnetic field δB_w by using Eq. (36)

$$\alpha_i = \gamma \frac{\int_w dV \delta B_w \mid \vec{\nabla} z \mid K_i^\dagger}{\omega_i \int_w dV \mid \vec{\nabla} z \mid K_i K_i^\dagger} \tag{40}$$

From Eqs. (39) and (40), we observe that the perturbed current on the resistive wall is actually proportional to the growth rate of the RWM. The substitution of Eq. (40) into Eq. (34) then gives

$$D_w = \frac{\gamma}{2} \sum_i \frac{(\int_w dV \mid \vec{\nabla} z \mid \delta B_w K_i)(\int_w dV \mid \vec{\nabla} z \mid \delta B_w K_i^\dagger)}{\omega_i \int_w dV \mid \vec{\nabla} z \mid K_i K_i^\dagger} \tag{41}$$

In the usual implementation for the computation of D_w, Eq. (37) is solved to obtain the set of eigenvalues ω_i and eigenfunctions K_i on the resistive wall. Then the form of D_w in Eq. (41) is evaluated to obtain the value of dissipation in terms of the perturbed magnetic field δB_w on the resistive wall.

There are several equivalent forms for D_w that are useful for one way or the other. First, we may use the definition of α_i in Eq. (40) to obtain an expression explicitly in terms of α_i

$$D_w = \frac{1}{2\gamma} \sum_i \omega_i \alpha_i^2 \int_w dV \mid \vec{\nabla} z \mid K_i K_i^\dagger \tag{42}$$

Next we may also express D_w in terms of the derivatives of K_i instead of K_i's by using the integral relations of K_i or Eq. (38) with $i = j$. We obtain the another expression

$$D_w = \frac{1}{2\gamma} \sum_i \alpha_i^2 \int_w \eta \vec{\nabla} K_i \cdot \vec{\nabla} K_i^\dagger (\mid \vec{\nabla} z \mid)^2 dV \tag{43}$$

A further application of the Eq. (38) allow us to change the single sum on α_i into a double sum, or

$$D_w = \frac{1}{2\gamma} \int_w \eta (\vec{\nabla} \sum_i \alpha_i K_i^\dagger)(\vec{\nabla} \sum_j \alpha_j K_j)(\mid \vec{\nabla} z \mid)^2 dV \tag{44}$$

Now by using the definition of K in Eq. (39), we obtain

$$D_w = \frac{1}{2\gamma} \int_w \eta \vec{\nabla} K \cdot \vec{\nabla} K^\dagger (\mid \vec{\nabla} z \mid)^2 dV \tag{45}$$

From Eq. (31), we can rewrite Eq. (45) as

$$D_w = \frac{1}{2\gamma} \int_w \eta \vec{j}^\dagger \cdot \vec{j} dV \tag{46}$$

Or the obvious result that D_w is the total amount of energy dissipated in the resistive wall.

B Examination of the Proposed Method by Application to One Dimensional Equilibria

In this appendix, we apply the proposed method given in Section II to the case of one dimensional equilibria and compare the results with known exact solutions to clarify the nature of the approximation. The exact one dimensional case we have in mind is the screw pinch [1] and/or the large aspect ratio cylindrical tokamak[26]. In this case the equilibrium

is only a function of r in the cylindrical coordinate (r, θ, z). All perturbed quantities can be assumed to be given by a single harmonic component with the phase factor $exp(im\theta + ikz)$, with m being the poloidal mode number and k the wave number in the z direction. The adjoint of the perturbed quantity would carry the complex conjugate phase factor. For simplicity, except where needed, we will drop the phase factor dependence of the perturbed quantities. For external kink modes, the potential energy of the plasma δW_p can be written as

$$\delta W_p = \frac{\pi L_z}{\mu_0} L_p \delta B_p^\dagger \delta B_p a \tag{47}$$

In Eq. (47), L_z is the length of the equilibrium in the z direction, and a is the radius of the plasma. δW_p is obtained from ideal MHD codes and Eq. (47) may be regarded as a definition for L_p. For the region between the plasma edge $r = a$ to the location of the resistive wall at $r = b$, the magnetostatic potential χ can be expressed as linear combinations of δB_p and δB_w with spatially dependent coefficients. In particular, at the plasma surface , we have

$$\chi_p = L_{pp} \delta B_p + L_{pw} \delta B_w. \tag{48}$$

At the inner edge of the resistive wall, we have

$$\chi_w^- = L_{wp} \delta B_p + L_{ww}^- \delta B_w \tag{49}$$

In Eqs. (48) and (49) the L coefficients are the reluctances. These reluctances depend on the geometry and mode numbers a, b, m, k. Their physical meaning can be obtained from the following considerations. For instance, for a perfect conducting wall, $\delta B_w = 0$, L_{pp} is the χ_p per unit δB_p. At the outer edge of the resistive wall, we have

$$\chi_w^+ = L_{ww}^+ \delta B_w \tag{50}$$

We note that if there are no current on the resistive wall, then $\chi_w^- = \chi_w+$, we may use Eqs. (49) and (50) to express δB_w in terms of δB_p. Substitution of it into Eq. (48) then gives us the relationship

$$\chi_p = (L_{pp} + \frac{L_{pw} L_{wp}}{L_{ww}^+ - L_{ww}^-}) \delta B_p \tag{51}$$

This situation is the same as if the external wall were infinitely far away $b = \infty$, we denote this as

$$\chi_p^\infty = L_{pp}^\infty \delta B_p \tag{52}$$

Note that with a resistive wall present, if $\chi_w^+ = \chi_w^-$, then the resistive wall does not carry any current, the distribution of the magnetic field is the same as if there were no wall or if the wall were at ∞. Comparison of Eqs. (51) with (52) gives the important identity that

$$L_{pp}^\infty = L_{pp} + \frac{L_{pw} L_{wp}}{L_{ww}^+ - L_{ww}^-} \tag{53}$$

With the expressions (48), (49), and (50), it is easy to evaluate the perturbed vacuum energy as

$$\delta W_v = \frac{\pi L_z}{\mu_0} [-L_{pp} a \delta B_p^\dagger \delta B_p - L_{pw} a \delta B_w^\dagger \delta B_p + L_{wp} b \delta B_p^\dagger \delta B_w + (L_{ww}^- - L_{ww}^+) b \delta B_w^\dagger \delta B_w] \tag{54}$$

Equation (36) may be solved for K in terms of δB_w as

$$K = \frac{\gamma \tau_w \delta B_w}{\mu_0 b(\frac{m^2}{b^2} + k^2)} \tag{55}$$

In Eq. (55), we have assumed that the toroidal wave number k is still much smaller than the poloidal wave number m/b and defined the resistive wall time τ_w as $\frac{db \cdot b \cdot \mu_0}{\eta}$. The dissipation functional is then obtained from Eq. (34) as

$$D_w = \frac{\pi L_z}{\mu_0} \frac{\gamma \tau_w \delta B_w^\dagger \delta B_w}{\frac{m^2}{b^2} + k^2} \tag{56}$$

The expression for δW_g is then given by

$$\begin{aligned}(L_p - L_{pp}) a \delta B_p^\dagger \delta B_p - L_{pw} a \delta B_w^\dagger \delta B_p + L_{wp} b \delta B_p^\dagger \delta B_w \\ + [(L_{ww}^- - L_{ww}^+) b + \frac{\gamma \tau_w}{\frac{m^2}{b^2} + k^2}] \delta B_w^\dagger \delta B_w = 0\end{aligned} \tag{57}$$

$$(L_p - L_{pp}) a \delta B_p + L_{wp} b \delta B_w = 0, \tag{58}$$

and

$$-L_{pw} a \delta B_p + [(L_{ww}^- - L_{ww}^+) b + \frac{\gamma \tau_w}{\frac{m^2}{b^2} + k^2}] \delta B_w = 0, \tag{59}$$

We may solve Eqs. (58) and (59) to obtain an expression for the growth rate

$$\gamma \tau_w = -\frac{\delta W_p + \delta W_{v\infty}}{\delta W_p + \delta W_{vb}} [(L_{ww}^- - L_{ww}^+) b (\frac{m^2}{b^2} + k^2)]. \tag{60}$$

This is an expression which is exact for cylindrical geometry and is of a very desirable form. The quantity in the square bracket is positive definite. Eq. (60) states that the RWM would have a positive growth rate if $\delta W_p + \delta W_{v\infty}$ is negative and $\delta W_p + \delta W_{vb}$ (δW_{vb} is δW_v with the ideal wall at b.) is positive, i.e. if the plasma is unstable to the external kink with the wall at infinite and stable with the wall being ideal. However, to apply this formula with results from the ideal stability codes, we also need results with $\delta W_p + \delta W_{vb}$. We note that with the wall at b the plasma is supposed to be stable to the ideal external kink. It is usually difficult for ideal MHD codes to compute this quantity when the plasma is stable. Therefore, we use Eq. (53) to express L_{pp} in terms of L_{pp}^∞ and obtain the expression

$$\gamma \tau_w = -[\frac{\delta W_p + \delta W_{v\infty}}{\delta W_p + \delta W_{v\infty} + \frac{L_z \pi a \delta B_p^\dagger \delta B_p}{\mu_0} \frac{L_{wp} L_{pw}}{L_{ww}^+ - L_{ww}^-}}] \cdot \frac{(L_{ww}^- - L_{ww}^+)(m^2 + k^2 b^2)}{b} \tag{61}$$

When we are close to marginal stability, we may ignore the first factor (the total amount of free energy available) in the denominator in the square bracket [] relative to the second one. This is the regime of parameter space where the present suggested approximation is valid. Since the total amount of free energy available is negative, this suggests that the proposed approximation is an under-estimation of the growth rate. An improved approximation could be obtained if we can evaluate the quantities separately and use the formula Eq.(61) directly. Although the derivations presented in the present section makes assumption about cylindrical geometry, much of the discussion is expected to remain valid for more general configurations with proper definitions of the reluctance coefficients. It is however worthwhile to use the

reluctance coefficients for the screw pinch to evaluate the quantities in Eqs. (60) and (61). For the screw pinch, it is easy to show that

$$L_{pp} = \frac{I_m(ka)K'_m(kb) - K_m(ka)I'_m(kb)}{k(Det)}, \tag{62}$$

$$L_{pw} = \frac{1}{k(Det)ka}, \tag{63}$$

$$L_{wp} = -\frac{1}{k(Det)kb}, \tag{64}$$

$$L^{-}_{ww} = \frac{K_m(kb)I'_m(ka) - I_m(kb)K'_m(ka)}{k(Det)}, \tag{65}$$

In Eqs. (62), (63), (64) and (65), k is the wavenumber in the z direction and

$$Det = I'_m(ka)K'_m(kb) - I'_m(kb)K'_m(ka) \tag{66}$$

and

$$L^{+}_{ww} = \frac{K_m(kb)}{kK'_m(kb)}, \tag{67}$$

I_m and K_m are the modified Bessel functions. In the large aspect ratio circular tokamak limit, we obtain the growth rate from Eq. (60) as

$$\gamma\tau_w = -\frac{\delta W_p + \delta W_{v\infty}}{\delta W_p + \delta W_{vb}} \frac{2(m^2 + k^2b^2)}{m[1 - (\frac{a}{b})^{2m}]} \tag{68}$$

whereas the evaluation of Eq.(61) gives

$$\gamma\tau_w = -\frac{\delta W_p + \delta W_{v\infty}}{\delta W_p + \delta W_{v\infty} + \frac{2L_z\pi a^2 \delta B_p^{\dagger}\delta B_p (a/b)^{2m}}{m\mu_0(1-(a/b)^{2m})}} \cdot \frac{2(m + k^2b^2/m)}{[1 - (a/b)^{2m}]} \tag{69}$$

It is quite obvious from comparing the expressions of Eq.(69) with Eq.(68) that the approximation proposed in Section II is valid when the factor $\delta W_p + \delta W_{v\infty}$ is small compared with the $\delta W_p + \delta W_{vb}$, or when the plasma is close to the unstable no wall limit and far from the stable ideal wall limit. We denote this as the situation when the RWM is weak.

C Calculation of $\delta\vec{B} \cdot \vec{n}$ in the KSTEP code

The KSTEP code was developed using on the stellarator expansion method and improved to include higher order corrections of toroidicity. This code is formulated with the flux surface based coordinates $(\Psi_{eq}, \theta, \phi)$. Here Ψ_{eq} denotes the equilibrium poloidal magnetic flux, and θ and ϕ are the toroidal and the poloidal angles, respectively. The poloidal angle θ is determined so that the magnetic field lines are straight lines in the $\theta - \phi$ plane. In this coordinate system, the effective equilibrium magnetic field $\vec{B}_{eq}$ in the stellarator expansion method is written as

$$\vec{B}_{eq} = q(\Psi_{eq})\vec{\nabla}\Psi_{eq} \times \vec{\nabla}\theta + \vec{\nabla}\phi \times \vec{\nabla}\Psi_{eq}, \tag{70}$$

where $q(\Psi_{eq})$ denotes the safety factor. Similarly, the perturbed magnetic field $\delta\vec{B}$ in the plasma region is expressed as

$$\delta\vec{B} = \vec{\nabla}\phi \times \vec{\nabla}\tilde{\Psi}. \tag{71}$$

The perturbed poloidal flux $\tilde{\Psi}$ is given by

$$\tilde{\Psi} = \left(\frac{R}{R_0}\right)^2 \vec{B}_{eq} \cdot \vec{\nabla}\Phi, \tag{72}$$

where Φ denotes a stream function which is related to the displacement vector $\vec{\xi}$ as

$$\vec{\xi} = \left(\frac{R}{R_0}\right)^2 \vec{\nabla}\phi \times \vec{\nabla}\Phi. \tag{73}$$

Since the normal vector $\vec{n}$ is given by $\vec{n} = \vec{\nabla}\Psi_{eq}/|\vec{\nabla}\Psi_{eq}|$, the normal component of the perturbed magnetic field is given by

$$\delta\vec{B} \cdot \vec{n} = -\frac{1}{\mathcal{J}|\vec{\nabla}\Psi_{eq}|}\frac{\partial}{\partial\theta}\left[\left(\frac{R}{R_0}\right)^2 \frac{1}{\mathcal{J}}\left(\frac{\partial}{\partial\theta} + q\frac{\partial}{\partial\phi}\right)\Phi\right], \tag{74}$$

where $\mathcal{J}$ denotes the Jacobian of the flux coordinates. The KSTEP code solves the eigenvalue equation for the stream function Φ. By substituting the eigenfunction Φ into Eq. (74) at the plasma boundary, we obtain the magnetic field normal to the plasma boundary.

References

[1] J.P. Freidberg, Ideal Magnetohydrodynamics New York: Plenum p.309, (1987).

[2] E.J. Strait, J.M. Bialek, N. Bogatu, M.S. Chance, M.S. Chu, D.H. Edgell, A.M. Garofalo, G.L. Jackson, R.J. Jayakumar, T.H. Jensen, O. Katsuo-Hopkins, J.S. Kim,R.J. LaHaye,L.L. Lao, M.A. Navratil, M. Okabayashi, H. Reimerdes, J.T. Scoville, A.D. Turnbull and DIII-D Team Phys. Plasmas , **11**, 2505 (2004).

[3] A. Bondeson, and D.J. Ward Phys. Rev. Lett., **72** 2709 (1994).

[4] T.H. Jensen and R. Fitzpatrick Phys. Plasmas, **4** 2997 (1997).

[5] Y.Q. Liu, and A. Bondeson, C.M. Fransson, B. Lennartson, and C. Breitholtz Phys. Plasmas, **7** 3681 (2000).

[6] A.M. Garofalo, A.D. Turnbull, M.E. Austin, J. Bialek, M.S. Chu, K. Comer, E.D. Fredrickson, R.J. Groebner, R.J. LaHaye, L.L. Lao, G.A. navratil, B.W. Rice, S.A. Sabbagh, J.T. Scoville, E.J. Strait, and T.S. Taylor Phys. Rev. Lett., **82** , 3811 (2003).

[7] A.D. Turnbull, D.P. Brennan, M.S. Chu, L.L. Lao, J.R. Ferron, A.M. Garofalo, P.B. Snyder, J. Bialek, I.N. Bogatu, J.D. Callen, M.S. Chance, K. Komer, D.H. Edgell, S.A. Galkin, D.A. Humphreys, J.S. kim, R.J. LaHaye, T.C. Luce, G.A. Navratil, M. Okabayashi, T.H. Osborne, B.W. Rice, E.J. Strait, T.S. Taylor, and H.R. Wilson Nucl. Fusion, **42** , 917 (2002).

[8] M.S. Chu, M.S. Chance, A.H. Glasser and M. Okabayashi Nucl. Fusion, **43**, 441 (2003).

[9] A.H. Glasser and M.S. Chance Bulletin of American Physical Society, **42**, 1848 (1997).

[10] M.S. Chance Phys. Plasmas, **4**, 2161 (1997).

[11] M.S. Chance, M.S. Chu, M. Okabayashi, and A.D. Turnbull Nucl. Fusion, **42**, 295 (2002).

[12] A. Iiyoshi, M. Fujiwara, M. Motojima, N. Ohyabu, and K. Yamazaki, Fusion Technology, **17**, 169 (1990).

[13] G. Grieger, W. Lortz, P. Merkel, J. Nuhrenberg, J. Sapper, E. Strumberger, H. Wobig, W7-X team, R. Burhenn, U. Gasparino, L. Giannone, H.J. Hartfuss, R. Jaenicke, G. Kuhner, H. Ringler, A. Weller, F. Wagner and the W7-AS Team, Physics of Fluids, **B4**, 2081 (1992).

[14] G.H. Neilson, M.C. Zarnstorff, J.F. Lyon, and the NCSX Team J. Plasma and Fusion Research, **78**, 214 (2002).

[15] K. Nishimura, K. Matsuoka, M. Fujiwara, K. Yamazaki, J. Todoroki, T. Kamimura, T. Amano, H. Sanuki, S. Okamura, M. Hosokawa, H. Yamada, S. Tanahashi, S. Kubo, Y. Takita, T. Shoji, O. Kaneko, H. Iguchi, and C. Takahashi Fusion Technology, **17**, 86 (1990).

[16] D. Anderson, W.A. Copper, R. Gruber, S. Merazzi, and U. Schwenn Scientific Computing, **II**, 159 (1990).

[17] C. Nuhrenberg Phys. Plasmas, **6**, 137 (1999).

[18] G. Anania, and J.L. Johnson Phys. Fluids, **26**, 3070 (1983).

[19] Y. Nakamura, K. Ichiguchi, M. Wakatani, and J.L. Johnson J. of Physical Society Japan, **58**, 3157 (1989).

[20] Y. Nakamura, M. Wakatani, and K. Ichiguchi, J. of Plasma and Fusion Research , **69**, 41 (1993).

[21] P. Merkel, C. Nührenberg, E. Strumberger, 31st EPS Conference on Plasma Phys. London, 28 June - 2 July 2004 ECA Vol.**28G**, P-1.208 (2004).

[22] I. Bernstein, E.A. Frieman, M.D. Kruskal, R. Kulsrud Proc. R. Soc. Ser., **A244**, 17 (1958).

[23] S.P. Hirshman, U. Schwenn, and J. Nuhrenberg J. Comput. Phys., **87**, 396 (1990).

[24] O. Motojima et. al. in Fusion Energy 2004 (Proc. 20th Int. Conf. Vilamoura, 2004) (Vienna: IAEA) CD-ROM file OV/1-4 and http://www-naweb.iaea.org/napc/physics/fec/fec2004/datasets/index.html

[25] Y. Nakamura, T. Matsumoto, M. Wakatani, S.A. Galkin, V.V. Drozdov, A.A. Martynov, Yu.Yu. Poshekhonov, K. Ichiguchi, L. Garcia, B.A. Carreras, C. Nührenberg, W.A. Cooper, and J.L. Johnson, J. of Comp. Phys., **128**, 43 (1996).

[26] M. Okabayashi, N. Pomphrey, R.E. Hatcher, Nuclear Fusion , **38** , 1607 (1998).